Radiation forces on a Rayleigh dielectric sphere in a patterned optical near field

Romain Quidant

ICFO-Institut de Ciències Fotòniques, Jordi Girona, 29, 08034 Barcelona, Spain

Dmitri Petrov

ICFO-Institut de Ciències Fotòniques, Jordi Girona, 29, 08034 Barcelona, Spain, and Institució Catalana de Recerca i Estudis Avançats, Barcelona, Spain

Gonçal Badenes

ICFO-Institut de Ciències Fotòniques, Jordi Girona, 29, 08034 Barcelona, Spain

Received November 12, 2004

We report on the study of the radiation forces exerted on a Rayleigh dielectric particle by a patterned optical near-field landscape at an interface decorated with resonant gold nanostructures. This configuration allows for the generation of a large array of surface subwavelength optical traps from an extended collimated beam, which may be of interest for parallel optical manipulation and sorting of submicrometer objects. © 2005 Optical Society of America

OCIS codes: 140.7010, 240.6690, 260.3910.

One of the current remaining challenges of so-called optical tweezers is the direct manipulation of objects with sizes that belong to the subwavelength (sub-λ) or Rayleigh regime. Indeed, the diffraction limit prevents one from achieving a commensurable trapping volume and thus does not allow for minimizing the fluctuation amplitude of the trapped object because of its strong Brownian motion. To overcome this limitation, it has been proposed to use evanescent fields instead of the usual propagating fields.[1–3]

The experimental observation of solid micrometer-sized dielectric and metallic particle manipulation in an extended homogeneous evanescent field has been reported both at the surface of a prism illuminated under total internal reflection and on top of an optical waveguide.[1,4–7]

The total radiation force upon a homogeneous surface wave contains two components: a scattering force parallel to the interface, induced by a change in the Poynting vector, and the gradient force toward the interface, which results from the optical field gradient. Because the scattering force pushes the particle along the incident in-plane wave vector, a homogeneous surface wave from an asymmetric illumination does not permit stable trapping but results in guiding along the surface. Trapping a particle at an interface thus requires additional confinement of the field in the interface plane.[8] Several configurations recently were studied theoretically to provide a three-dimensional subwavelength optical trapping volume.[2,9,10]

The latest advances in optics of noble-metal nanostructures have provided new configurations for achievement of nano-optical tweezers. In particular, tightly localized modes resulting from the strong near-field coupling between two closely spaced metallic nanoparticles lead to a stable trap for a single fluorescent molecule.[11] Nevertheless, the high sensitivity of these modes to the interparticle gap[12] renders this configuration difficult to control with current fabrication techniques.

Quidant *et al.* recently demonstrated the possibility of patterning the optical near field at a surface decorated by a matrix of resonant gold nanopads.[13] Under suitable conditions the in-plane far-field coupling between the gold dots gives rise to an extended array of reproducible interpad sub-λ intensity maxima. Here we calculate the radiation forces on Rayleigh dielectric spheres induced by such an optical near-field landscape and investigate their capability for optical trapping. Our system, shown in Fig. 1, consists of a two-dimensional square matrix of gold nanopads lying upon a heavy flint glass prism ($n_{pr}=1.80$) and immersed in water ($n_a=1.33$). The gold nanopads are parallelepipeds with 100-nm sides and 20-nm height; the pitch of the grating is fixed at 640 nm. The illumination is performed under total internal reflection (incident angle, $\theta=80°$) with a p-polarized plane wave. We calculated the distribution of the electric near-field intensity above the decorated surface by using the Green dyadic method. Such a method, which requires only specification of the dielectric function and of the geometry of the scattering centers, has proved to be well suited for modeling the interaction of light with plasmonic nanosystems.[14]

Figure 2(a) shows the distribution of the square modulus of the electric field in a plane parallel to the

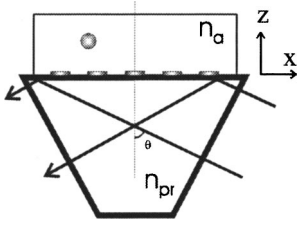

Fig. 1. Schematic of the optical configuration.

0146-9592/05/091009-3/$15.00

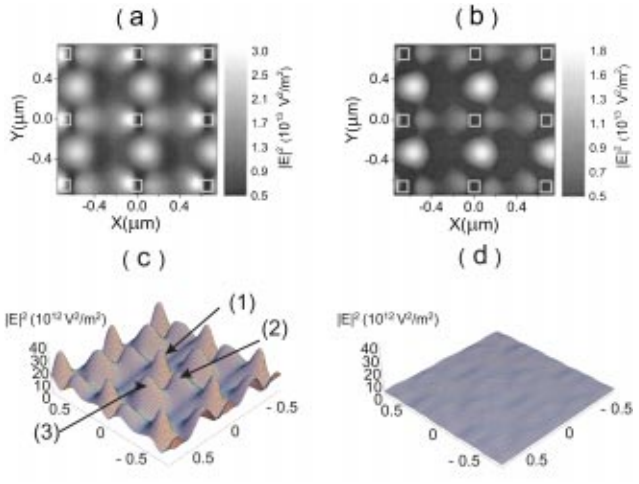

Fig. 2. Distribution of the square modulus of the electric field at the LSP resonance ($\lambda = 840$ nm): (a) at $Z = 100$ nm and (b) at $Z = 150$ nm. The three-dimensional views illustrate the change of contrast when the illumination is (c) resonant and (d) nonresonant ($\lambda = 514$ nm).

surface ($Z = 100$ nm) when the incident wavelength matches the localized surface plasmon (LSP) resonance of each of the gold pads ($\lambda = 840$ nm). Under the illumination conditions considered, the local field around the gold dots displays two intensity maxima [types (1) and (2)] aligned along the incident in-plane wave vector, which are similar to what is observed for isolated pads. At this height the map is also dominated by an additional periodic pattern of interpad maxima [type (3)] that result from the far-field coupling between the LSP fields. The average (FWHM) diameter of the interpad spots is ~ 200 nm, i.e., smaller than one quarter of the incident wavelength. Their transverse confinement (along the Z axis) is defined mainly by the decreasing exponential tail of the incident evanescent field (200 nm at $1/e^2$) and thus extends further than the LSP fields around the pads, as can be seen in Fig. 2(b). Of the three types of maxima, only type (3) shows the symmetrical profile required for potential stable trapping. The contrast of the near-field landscape is dramatically reduced by a factor of 2.56 when the illumination wavelength ($\lambda = 514$ nm) is away from the LSP resonance band [Figs. 2(c) and 2(d)]. Under these conditions the gold pads act as low-scattering perturbations that just slightly modify the homogeneous distribution of the incident wave.

The field pattern under resonance provides a periodic optical potential landscape that may influence the dynamics of a small object located close to the surface. In what follows, we evaluate the optical forces exerted on a dielectric nanosphere of refractive index n_p. As long as the nanosphere's radius R is kept small compared with the incident wavelength, the gradient $F^{(i)}_{\mathrm{grad}}$ and scattering $F^{(x)}_{\mathrm{scat}}$ forces can be calculated under the dipole approximation for which analytical formulas are available[15]:

$$F^{(i)}_{\mathrm{grad}} = \pi n_a^2 \epsilon_0 R^3 \frac{m^2-1}{m^2+1} \frac{d|E(x,y,z)|^2}{dx_i},$$

$$F^{(x)}_{\mathrm{scat}} = \frac{8}{3} \frac{n_a n_{pr} \sin\theta\, \epsilon_0}{2} \pi (kR)^4 R^2 \left(\frac{m^2-1}{m^2+1} \right)^2 |E(x,y,z)|^2,$$

where n_a and n_{pr} stand for the refractive indices of water and of the substrate, respectively, ϵ_0 is the dielectric constant of vacuum, $k = 2\pi/\lambda$, and $m = n_a/n_p$. In these expressions the electric field $|E(x,y,z)|^2$ does not account for the multiple reflections between the dielectric particle and the interface. This approximation stays valid, provided that the particle size does not exceed one third of the incident wavelength and that the particle is located at a larger distance from the surface than the particle radius.[3,9]

Figure 3 plots the projection in the X–Y plane of the total force distribution exerted on a 50-nm-radius polystyrene particle ($n_p = 1.55$) for an incident field intensity of $I = 10^{11}$ W/m^2. At $Z = 100$ nm, three different regions of significant force, corresponding to the field maxima observed in Fig. 2(a), can be distinguished. Near the gold pad locations [positions (1) and (2)], the force distribution is nonsymmetric and does not provide a stable trap for the nanosphere. The interpad spots [position (3)], however, correspond to symmetric radial force vectors of maximum amplitude 0.58 pN that vanish at the central location of highest field intensity. As expected from the field map of Fig. 2(b), at a slightly higher plane ($z = 150$ nm) the force magnitude at positions (1) and (2) becomes insignificant compared with that of position (3). The evolution of the total force in vertical plane X–Z for $Y = 320$ nm (Fig. 4) indicates that the localized wells are formed ~ 400 nm from the interface. Consequently a Rayleigh particle approaching the surface

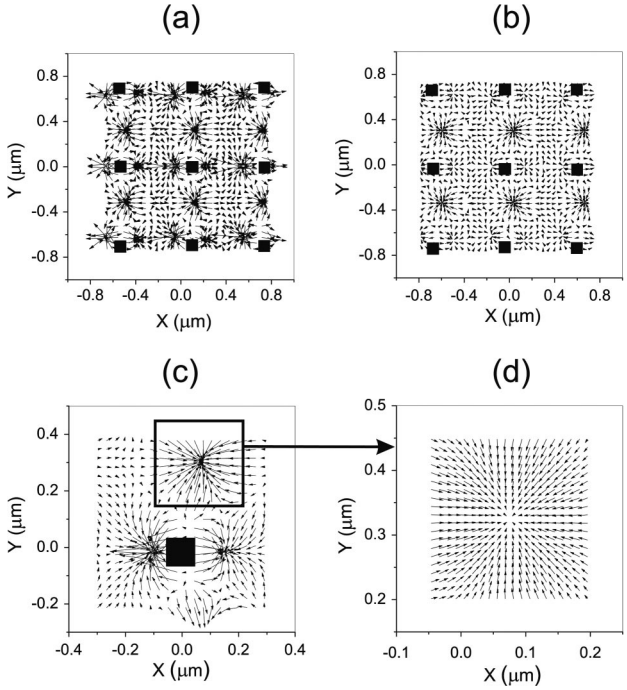

Fig. 3. Distribution in the X–Y plane of the total radiation force exerted on a dielectric sphere ($n_p = 1.55$) with radius $R = 50$ nm at (a) $Z = 100$ nm and (b) $Z = 150$ nm. (c), (d) Magnified views of map (a).

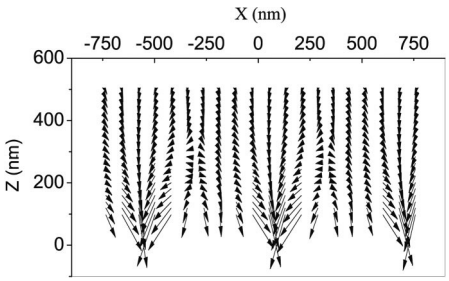

Fig. 4. Radiation force distribution in the plane X–Z along a line of stable traps (Y=320 nm).

will go down at these positions and should stabilize there preferentially before being influenced by the field around the gold pads. As expected, on nonresonant illumination λ=514 nm, the force magnitude is weak and is defined mainly by the scattering force contribution 0.015 pN (not shown here for the sake of brevity).

The practical trapping ability of the sub-λ interpad spots depends on whether the resultant optical forces exceed other forces that affect the movement of the trapped particle. The main contributions come from the Brownian motion that is due to the collisions of molecules of the ambient medium and from their gravitation. We do not consider here other specific forces that depend on the physical–chemical state of the interface, such as the electrostatic force. The gravitation force is given by $F_g=(4/3)\pi R^3 g\rho$, where g is the gravitational acceleration and $\rho=1.056\ g\ \mathrm{cm}^{-3}$ is the density of the polystyrene. One can estimate the effect of Brownian motion in an optical trap by comparing thermal energy k_BT with potential U of the gradient force $F_{\mathrm{grad}}^{(i)}=-\mathrm{grad}U$.[16] This estimation shows that, for a particle radius larger than 27 nm, the optical potential overcomes the thermal and gravitational energies and the particle is maintained at the center of the trap.

To summarize, the optical near field at the vicinity of a surface patterned with a matrix of resonant gold nanopads leads to a periodic optical potential landscape for Rayleigh dielectric objects. The radiation force map is characterized by potential wells located between the gold nanostructures, where a dielectric bead may be attracted and preferentially may stay because of the presence of significant gradient forces. This configuration opens the possibility of creating arbitrary arrangements of trapping sites for self-assembly. Also, the surface optical potential created should allow for the extension of the microfluidic sorting scheme described in Ref. 17 to nanometer-scale entities.

This research was carried out in the framework of the European Science Foundation (Eurocores on Sons) through grant 02-PE-SONS-063-NOMSAN and with the financial support of the Spanish Ministry of Education and Science. R. Quidant's e-mail address is romain.quidant@icfo.es.

References

1. S. Kawata and T. Suguira, Opt. Lett. **17**, 772 (1992).
2. L. Novotny, R. X. Bian, and X. S. Xie, Phys. Rev. Lett. **79**, 645 (1997).
3. M. Nieto-Vesperinas, P. Chaumet, and A. Rahmani, Philos. Trans. R. Soc. London Ser. A **362**, 719 (2004).
4. S. Kawata and T. Tani, Opt. Lett. **21**, 1768 (1996).
5. K. Sasaky, M. Tsukima, and H. Masuhara, Appl. Phys. Lett. **71**, 37 (1997).
6. K. Wada, K. Sasaki, and H. Masuhara, Appl. Phys. Lett. **76**, 2815 (2000).
7. K. Sasaki, J. Hotta, K. Wada, and H. Masuhara, Opt. Lett. **25**, 1385 (2000).
8. M. Gu, J. B. Haumonte, Y. Micheau, J. W. M. Chon, and X. Gan, Appl. Phys. Lett. **84**, 4236 (2004).
9. P. Chaumet, A. Rahmani, and M. Nieto-Vesperinas, Phys. Rev. Lett. **88**, 123601 (2002).
10. K. Okamoto and S. Kawata, Phys. Rev. Lett. **83**, 4534 (1999).
11. H. Xu and M. Kall, Phys. Rev. Lett. **89**, 246802 (2002).
12. J. P. Kottmann and O. J. F. Martin, Opt. Express **8**, 655 (2001); http://www.opticsexpress.org.
13. R. Quidant, G. Badenes, S. Cheylan, R. Alcubilla, J.-C. Weeber, and Ch. Girard, Opt. Express **12**, 282 (2004), http://www.opticsexpress.org.
14. J. R. Krenn, A. Dereux, J. C. Weeber, E. Bourillot, Y. Lacroute, J. P. Goudonnet, G. Schider, W. Gotschy, A. Leitner, and F. R. Aussenegg, Phys. Rev. Lett. **82**, 2590 (1999).
15. Y. Harada and T. Asukura, Opt. Commun. **124**, 529 (1996).
16. A. Ashkin, J. M. Dziedzic, J. E. Bjorkholm, and S. Chu, Opt. Lett. **11**, 288 (1986).
17. M. P. MacDonald, G. C. Spalding, and K. Dholakia, Nature **426**, 421 (2003).